Chinese Herbal Medicines 13 (2021) 370–380

Contents lists available at ScienceDirect

Chinese Herbal Medicines

journal homepage: www.elsevier.com/locate/chmed

Original Article

Self-assembled aggregations in *Coptidis Rhizoma* decoction dynamically regulate intestinal tissue permeability through Peyer's patch-associated immunity

Qing-qing Zhang [a], Ye Yang [a,b,c,d,*], Rong-rong Ren [a], Qing-qing Chen [a], Jing-jing Wu [a], Yu-yu Zheng [a], Xiao-hui Hou [a], Yu-feng Zhang [a], Ming-song Xue [a], Deng-ke Yin [a,b,c,*]

[a] *School of Pharmacy, Anhui University of Chinese Medicine, Hefei 230012, China*
[b] *Institute of Pharmaceutics, Anhui Academy of Chinese Medicine, Hefei 230012, China*
[c] *Engineering Technology Research Center of Modernized Pharmaceutics, Education Office of Anhui Province, Hefei 230012, China*
[d] *State Key Laboratory of Natural Medicines, China Pharmaceutical University, Nanjing 210009, China*

ARTICLE INFO

Article history:
Received 28 June 2020
Revised 13 October 2020
Accepted 13 December 2020
Available online 30 June 2021

Keywords:
Coptidis Rhizoma decoction
intestinal absorption
intestinal mucosal immunity
Peyer's patches
self-assembled aggregations

ABSTRACT

Objective: To investigate the dynamic regulation of self-assembled aggregations (SAA) in *Coptidis Rhizoma* decoction on the permeability of intestinal tissue and the mechanism underlying.
Methods: The effects of SAA on berberine (Ber) absorption were respectively analyzed in an in situ intestinal perfusion model and in an Ussing Chamber jejunum model with or without Peyer's patches (PPs). The expression levels of ZO-1, Occludin and Claudin-1 were detected by immunofluorescence to evaluate the tight junction (TJ) between intestinal epithelium cells. The expression levels of T-box-containing protein expressed in T cells, signal transducers and activators of tranion-6, retinoic acid receptor-related orphan receptor γt and forkhead box P3 in PPs were detected by the reverse transcription-polymerase chain reaction and the secretions of interferon-γ (IFN-γ), interleukin-4 (IL-4), interleukin-17 (IL-17) and transforming growth factor-β (TGF-β) in PPs were evaluated by immunohistochemistry, to reflect the differentiation of T lymphocyte in PPs to helper T (Th) cell 1, Th2, Th17 and regulatory T (Treg) cell. To confirm the correlation between SAA in *Coptidis Rhizoma* decoction, PPs-associated immunity and intestinal epithelium permeability, SAA were administrated on an Ussing Chamber jejunum model with immunosuppressed PPs and evaluated its influences on intestinal tissue permeability and TJ proteins expression.
Results: SAA in *Coptidis Rhizoma* decoction could dose-dependently promote Ber absorption in jejunum segment, with the participation of PPs. The dose-dependent and dynamical regulations of SAA on permeability of intestinal tissue and TJ proteins expression level between intestinal epithelium cells occurred along with the dynamically changed T lymphocyte differentiation and immune effectors secretion in PPs. The administration of SAA on immunosuppressed PPs exhibited dose-dependent PPs activation, inducing dynamic promotion on intestinal tissue permeability and inhibition on TJ proteins expression.
Conclusion: SAA can improve the Ber absorption in small intestine, through the PPs-associated immunity induced dynamic regulation on intestinal tissue permeability and TJ proteins expression. These findings might enlighten the research of traditional Chinese medicine decoction.

1. Introduction

Decoction is one of the earliest and most widely used dosage forms in traditional Chinese medicine (TCM) (Huang et al., 2019). During the decoction process, it doesn't just have the dissolving of active small molecules, it also has the dispersion of biological macromolecules, especially the polysaccharide molecules in herbal medicines. The polysaccharide macromolecules dispersed in decoction will self-assemble into a colloid form during cooling and standing (Zhuang et al., 2008). The medicine residues in the decoction will be removed by gauze filtration before taking, but the dispersed polysaccharide aggregates will be taken along with the active ingredients (Liu & Huang, 2019; Shi, Lin, & Yao, 2018). *Coptidis Rhizoma* is one of the most widely used TCM in clinic, with berberine (Ber) as the main active ingredient (Wang et al., 2019; Xiao et al., 2020). Previous studies have shown that the *Coptidis*

* Corresponding authors.
E-mail addresses: Y.Yang@ahtcm.edu.cn (Y. Yang), yindengke@ahtcm.edu.cn (D.-k. Yin).

https://doi.org/10.1016/j.chmed.2021.06.004
1674-6384/

Rhizoma decoction always exhibit better bioavailability of Ber than that of Ber solution (Jiao, Hou, Yin, Yang, & Gui, 2016; Li et al., 2019; Meng et al., 2018). Does this unique phenomenon in the *Coptidis Rhizoma* decoction related to the colloidal aggregations formed by polysaccharide macromolecules?

Intestine is the largest immune organ in human body, carrying>70% of immune cells (Filipp, Brabec, Vobořil, & Dobeš, 2019). The Micro-fold cells (M cells) on the surface of Peyer's patches (PPs) are the important immune-inducing sites in the intestinal mucosal immune system, which can transfer the immunogenic macromolecules to the immune cells in the lymphatic follicles below (Rathan et al., 2019). Intestinal mucosal immunity is one of the major regulators of the tight junction (TJ) between intestinal epithelium cells and improves paracellular permeability (Lin et al., 2019). In recent years, many kinds of polysaccharides had been found to have multiple immune activities, and some of them had been used as the adjuvant of vaccine (Gu et al., 2019; Guo et al., 2019; Liu et al., 2019). The oral vaccines with polysaccharides as carrier materials can be uptaken by the M cells of intestinal PPs, then activate the intestinal immune system (Brayden, Jepson, & Baird, 2005; Zhou et al., 2017). Our previous studies have confirmed that the self-assembled aggregations (SAA) in the *Coptidis Rhizoma* decoction are mainly composed of *Coptidis Rhizoma* polysaccharides (CCP), which contains 32.76% total sugar, 35.74% uronic acid and 0.24% protein, and composites monosaccharide of galacturonic acid, arabinose, galactose and rhamnose (Yang, Li, Yin, Chen, & Gao, 2016). Does the excellent bioavailability of Ber in *Coptidis Rhizoma* decoction related to the immune activity of the CCP composed SAA?

In this study, the effects of SAA on intestinal Ber absorption and the immunological mechanism underlying were studied. To avoid the disturbances from other intestinal segments, intestinal contents, and intestinal flora, isolated intestinal tissue models, with or without PPs, were established by an Ussing Chamber System. The present study was aimed to lay a scientific foundation for the further development and utilization of the conventional dosage form of TCM.

2. Materials and methods

2.1. Chemical reagents

Ber (purity > 99%) was acquired from Shanghai Yuanye Biotechnology Co., Ltd (Shanghai, China). Rabbit anti-rat antibodies specific to interferon-γ (IFN-γ, bs-0480R), interleukin-4 (IL-4, bs-0581R), interleukin-17 (IL-17, bs-1183R) and transforming growth factor-β (TGF-β, bs-0086R), polymer detection system kit (PV-6000) and 3,3′-diaminobenzidine (DAB) were purchased from Bioss Biosynthesis Biotechnology Co., Ltd (Beijing, China). The primary rabbit antibodies against ZO-1 (PB9234), Occludin (bs-10011R) and Claudin-1 (CSB-PA001656) were purchased from Boster Biological Technology Co., Ltd (Wuhan, China), Bioss Biosynthesis Biotechnology Co., Ltd (Beijing, China) and Cusabio Biotech Co., Ltd (Wuhan, China), respectively. All other chemicals and solvents were analytical grade and obtained from Zhongshi Chemical Engineering Company (Shanghai, China).

2.2. Animals

The Sprague-Dawley rats (SD male rats; 180–200 g; age, 5 months), which were supplied by the Experimental Animal Center of Anhui Medical University (Anhui, China) were allowed to acclimatize for at least one week before experimentation, fed with a standard diet and allowed water ad libitum. Procedures for the use of experimental animals conformed to the Guide for the Care and Use of Laboratory Animals and were approved by the experimental animal ethics committee of Anhui University of Chinese Medicine.

2.3. Preparation of SAA

The medicine material of *Coptidis Rhizoma* was obtained from Anhui Anbao Medicinal Materials Company (Lot No. 20160811, Anhui, China) and identified by Professor Shou-jin Liu (School of Pharmacy, Anhui University of Chinese Medicine, China), in accordance with the *China Pharmacopoeia* (2015). Briefly, *Coptidis Rhizoma* was weighed and immersed into distilled water with ratio of 1:10 (mass to volume). After decocting for 90 min, the residue was removed by multi-step filtrations of gauze, filter pulp and filter paper to obtain the *Coptidis Rhizoma* decoction (Xu et al., 2018). The decoction was centrifuged at high speed, washed with distilled water, and then centrifuged to collect SAA.

2.4. Characterization of SAA

The composition of SAA was analyzed, and SAA was dissolved in 1 mol/L NaOH solution. The content of macromolecular substances (polysaccharide and protein) in SAA was determined by phenol–sulfuric acid method (Xue, Tong, Wang, & Liu, 2018) and coomassie brilliant blue method (Biundo, Reich, Ribitsch, & Guebitz, 2018) respectively.

A high-performance liquid chromatography (HPLC) method was established to determine the content of Ber in *Coptidis Rhizoma* decoction and SAA. Firstly, the Ber standard and SAA were accurately weighed, and then Ber solution (100 μg/mL) and SAA suspension (120 μg/mL) were prepared with methanol. Secondly, the *Coptidis Rhizoma* decoction, Ber solution and SAA solution were filtered using a 0.45 μm syringe filter respectively and analyzed with an HPLC system, including a Waters 2707 sample injector (Milford, MA), a Waters 2695 separations module (Milford, MA), a Hypersil BDS C_{18} column (200 mm × 4.6 mm × 5.0 μm, Hypersil, Runcorn, U.K.) as the analytical column, a mixed solution of acetonitrile and 0.1% phosphoric acid solution (45 : 55, volume percentage) as the mobile phase at a flow rate of 1.0 mL/min, temperature at 25 °C, and a Waters 2487 dual absorbance ultraviolet detector (Milford, MA) at a detected wavelength of 265 nm.

Considering the dose of SAA content in *Coptidis Rhizoma* decoction, SAA was weighed accurately and suspended with distilled water to 17 mg/mL. The morphology of SAA was observed using transmission electron microscope (TEM, JEM2010, Japan) at an acceleration voltage of 80.0 kV. The size distribution and surface potential of SAA were detected using a dynamic light scattering (DLS, Zetasizer Nano 2S90, Malvern, U.K.) at 25 °C after ultrasonic dispersion. All data were obtained from the average of three measurements.

2.5. Intestinal perfusion experiment

The intestinal perfusion model was established to analyze the effect of SAA on Ber absorption. According to our previous report, the jejunum segment was the advantage position of Ber absorption and was selected for the next experiments (Jiao et al., 2016). The experiments were divided into groups of Ber, Ber-SAA_L, Ber-SAA_M and Ber-SAA_H. The dose of SAA was established based on the dose of *Coptidis Rhizoma* in clinic for treating enteritis and the SAA content in decoction. The dose of Ber was based on the oral dose in clinic relevant experimental literature (Deng & Song, 2019; Jiao et al., 2016). All the rats were fasted for 12 h (free drinking water) before experiments. The rats were anesthetized by intraperitoneal injection of 20% urethane solution (6 mL/kg) (Sun et al., 2016). After fixation, 2–3 cm incision was opened along the midline of the abdomen. A jejunum segment of about 10 cm was selected, and the incisions at both ends were inserted into a rubber tube and ligated. The intestinal contents were gently removed with pre-warmed saline and perfused with 40 mL of perfusate at a rate

of 0.2 mL/min using a constant current pump (HL-1, HuXi®, Shanghai, China). The Ber group was perfused with Ber solution (100 μg/mL), and the other three groups were perfused with Ber solutions (100 μg/mL) containing low- (SAA_L, 40 μg/mL), medium- (SAA_M, 80 μg/mL), and high-dose (SAA_H, 120 μg/mL) of SAA. After 1 h of perfusion, the perfusion solution was taken out and the content of Ber was determined by fluorescence spectrophotometer (F-4600, Hitachi, Japan). The absorption rate constant (K_a) and the apparent absorption coefficient (P_{app}) of Ber was calculated by the following formulas.

$$K_a = \frac{Q}{\pi r^2 l} \times \left(1 - \frac{C_{out} V_{out}}{C_{in} V_{in}}\right) \quad (1)$$

$$P_{app} = -\frac{Q}{2\pi r l} \times \ln \frac{C_{out} V_{out}}{C_{in} V_{in}} \quad (2)$$

where V_{in} and V_{out} were the perfusate volumes of the inlet and outlet perfusate (mL), respectively; C_{in} and C_{out} were the concentrations of Ber at the inlet and outlet (μg/mL), respectively; Q was the perfusion velocity (mL/min); And l and r were the length and the radius of the perfusion intestine segments, respectively.

2.6. Establishment of immunosuppressed rat model

In order to further investigate whether SAA affect jejunal epithelium permeability through PPs-associated immunity, an immunosuppressed rat model was established by intraperitoneal injection with cyclophosphamide at 80 mg/kg/d for 6 d (Wang et al., 2012; Yang, Kim, Kang, Lee, & Park, 2018).

2.7. Using Chamber experiment

In order to avoid the influence of other intestinal segments, intestinal contents and intestinal flora, an Ussing Chamber jejunum model with or without PPs was established for experiment. To investigate whether the effect of SAA on Ber permeation was related to PPs, the experiments were divided into groups of NPPs (jejunum tissues without PPs), SAA_L-NPPs, SAA_M-NPPs, SAA_H-NPPs, PPs, SAA_L-PPs, SAA_M-PPs and SAA_H-PPs. Fluorescein (Flu) was used as a model drug for paracellular pathway absorption to observe the permeability of jejunal epithelium cells.

To confirm the immune activation of PPs on the permeability of jejunal epithelium cells, immunosuppressed PPs (PPs_{IP}) in jejunum was taken out from the immunosuppressed rat model and an Ussing Chamber jejunum model with or without PPs_{IP} was established for experiment (Jiang et al., 2019). The experiments were divided into PPs group (jejunum incubated with PPs at the serosa side), SAA-PPs groups (jejunum incubated with PPs and SAA at the serosa side) containing different dosages of SAA (SAA_L-PPs, SAA_M-PPs and SAA_H-PPs), PPs_{IP} group (jejunum incubated with PPs_{IP} at the serosa side), and SAA-PPs_{IP} groups (jejunum incubated with PPs_{IP} and SAA at the serosa side) containing different dosages of SAA (SAA_L-PPs_{IP}, SAA_M-PPs_{IP} and SAA_H-PPs_{IP}). Flu solution (100 μg/mL) was added on the mucosal side.

Firstly, the jejunums from anesthetized rats were immediately removed by surgery and washed with Krebs-Ringer solution (KR solution), and then placed in cold (on ice) and bubbled (O_2: CO_2 = 95:5) KR solution. Secondly, the jejunums were cut into 2 cm pieces, respectively, and serosas were removed by blunt dissection. The stripped tissues were mounted in chambers with exposed surface area of 0.5 cm^2. Five milliliter KR solution was added to both sides of the intestinal tissue (mucosal and serosal side) for 30 min equilibrium. Temperature of the chambers was maintained at (37 ± 0.5) °C. Tissue viability was continuously controlled by potential difference, and the tissue with electrical value < 2 mV was refused (Huang et al., 2018). After equilibration for 30 min, the KR solution on both sides was removed. Five milliliter of Ber or Flu solutions (100 μg/mL) containing low- (SAA_L, 40 μg/mL), medium- (SAA_M, 80 μg/mL), or high-dose (SAA_H, 120 μg/mL) of SAA was immediately added to the mucosal side, while the same volume of fresh KR solution was added to the serosa side. One-half milliliter sample was taken from the serosal side every 30 min, and an equal volume of KR solution was immediately added for replacement. The contents of Ber and Flu in the samples were detected by fluorescence spectrophotometer respectively. The accumulative quantity (A) and apparent permeability (P_{app}) were calculated by the following formulas. In the experiment without Ber and Flu, the experiments were finished after 30, 60, 90 and 120 min, respectively. The jejunal tissues and PPs of the above groups were taken and fixed with 4% paraformaldehyde. Paraffin sections were used for subsequent experiments (Huang et al., 2016; Li, Jin, Shim, & Shim, 2012). The jejunal tissues and PPs incubated with KR solution were set as BC group, while the jejunal tissues without any treatment was set as NC group. Because the area of the tissue clamp in the Ussing Chamber System is 0.5 cm^2, only one Peyer's patch can be fixed in a detection cell. But multiple detection cells can be tested in an Ussing Chamber System simultaneously. At each time point, suitable numbers of detection cells were removed from the Ussing Chamber System and the PPs were collected for subsequent analyses.

$$A = 5C_n + 0.5\sum_{i=1}^{n-1} C_i \quad (3)$$

$$P_{app} = \frac{dQ/dt}{a \times C_0} \quad (4)$$

where C_n (mmol/L) was the concentration of the drug at the time point (n), A (mmol/L) was the accumulated permeation amount, a was the exposed surface area of the intestine (0.5 cm^2), dQ/dt (mmol/L/s) was the amount of the drug transported, and C_0 (mmol/L) was the initial concentration of the test drug.

2.8. Immunohistochemical and immunofluorescence analysis

Tissue sections were incubated with primary antibodies against IFN-γ, IL-4, IL-17, TGF-β, ZO-1, Occludin and Claudin-1 at 4 °C overnight. Immunohistochemical sections were incubated in PV-6000, DAB showed hematoxylin staining, while immunofluorescence sections were incubated with Cy3 labeled secondary antibody, and then stained with DAPI. Photos were taken using a fluorescence microscope. In order to evaluate the expression levels of the target proteins, 10 areas under the 200 × field of vision were randomly selected, and the integrated optical density (IOD) was calculated by Image-pro Plus 6.0.

2.9. Western blotting (WB) analysis

Tissues were homogenized by a RIPA lysis buffer on ice, centrifuged at 12 000 rpm for 10 min, and determined the total protein content using a BCA protein assay kit (Thermo Fisher, USA). Each sample with 30 mg protein content was separated by a polyacrylamide gel electrophoresis and transferred onto a polyvinylidene fluoride (PVDF) membrane (Merck Millipore, Germany). The PVDF membrane was blocked using 5% BSA, incubated with primary antibodies against ZO-1, Occludin, Claudin-1 or GADPH, washed with Tris buffered saline tween, incubated with horse radish peroxidase-conjugated secondary antibodies, and visualized using diaminobenzidine. Images were collected using a UVsolo Touch Gel Imager (Analytik Jena AG, Germany) and the grey values were analyzed using the Image J software (Media Cybernetics, USA).

2.10. Reverse transcription polymerase chain reaction (RT-PCR)

In order to evaluate the differentiation of T lymphocytes to helper T (Th) cell 1, Th2, Th17 and regulatory T (Treg) cell, the expression levels of T-box-containing protein expressed in T cells (T-bet), signal transducers and activators of tranion-6 (STAT-6), retinoic acid receptor-related orphan receptor γt (ROR-γt) and forkhead box P3 (FoxP3) were used as indicators and their expression levels were analyzed semi-quantitatively by RT-PCR. Total RNA was extracted by homogenization of 100 mg PPs in 1 mL Trizol reagent (Invitrogen, Cergy, France) according to the manufacturer's suggested protocol, then semi-quantitative RT-PCR analysis were performed as previously described. Amplification products (10 μL of each) were separated by electrophoresis in a 2% TBE agarose gel stained with ethidium bromide. The fluorescence intensity of bands were determined with an Alpha Fluorchem Imager Gel Analysis System version 2.00 (Alpha Innotech Corporation, San Leandro, CA, USA). Design and synthesis of primer sequences were provided by Sangon Biotech Co., Ltd. (Shanghai, China). The primer sequences were shown in Table 1.

Ethical approval

All animal experiments were performed in compliance with the Animal Management Rules of the Ministry of Health of the People's Republic of China and the guidelines for the Care and Use of Laboratory Animals of Anhui University of Chinese Medicine. At the end of the experiments, all the animals were sent to the laboratory animal center for unified treatment. All efforts were made to minimize the suffering of animals and to reduce the number of animal use.

2.12. Statistical analysis

The number of animals in each experimental group was kept n = 5, and parallel groups in other experiments was performed three times. All the experiments were repeated at least three times. All the data were expressed as mean ± standard deviation (SD), and the statistical analysis were performed using one-way ANOVA followed by LSD post hoc test in the SPSS 24.0 software (SPSS, USA). Differences between the groups were considered statistically significant at $P < 0.05$, $P < 0.01$, and $P < 0.001$.

3. Results

3.1. Characterization of SAA

The yield of SAA was (1134 ± 10.72) mg/10 g crude medicine or (17.01 ± 0.86) mg/mL decoction. It was found that the main component of SAA was polysaccharide, which was consistent with the results of our previous studies (Jiao et al., 2016; Yang et al., 2016). Fig. 1A showed HPLC chromatograms of the *Coptidis Rhizoma* decoction, Ber solution and SAA solution. The results showed that Ber was not detected in SAA solution. Fig. 1B was the representative TEM image of SAA dispersed in water. The SAA had regular shape and cluster structure similar to crystal. DLS results showed that the SAA had size distribution of (423.72 ± 23.8) nm and zeta potential of (−3.70 ± 0.21) mV.

Table 1
Primer sequences used for RT-PCR reactions.

Genes	Sequences (5′- 3′)	cDNA PCR product /bp
T-bet	F[a] ACCGAGCCGATGCCGAGTG	365
	R[a] AGCTTCCCAGACACCTCCAACC	
STAT-6	F GCAGGCTTCAGCACCGAGTAAG	398
	R GGTTCGCAGGACTTCATCCAGAC	
FoxP3	F TGCTGTGCGGAGACACCTCTG	344
	R GGCGTTGGCTCCTCTTCTTGC	
ROR-γt	F AAGAAGACCCACACCTCACAAATCG	333
	R TTCCCGTTGCTGCTGCTGTTG	

[a] F, forward; R, reverse.

3.2. SAA significantly affected Ber absorption in small intestine

Fig. 1C showed the effect of SAA on Ber absorption in small intestine. In intestinal perfusion experiment, the Ber-SAA_M and Ber-SAA_H groups significantly promoted K_a and P_{app} of Ber absorption, compared with the Ber group ($P < 0.05$).

3.3. SAA significantly affected Ber permeation in isolated small intestinal tissues with PPs

Fig. 2 showed the effect of SAA on Ber permeation in isolated intestinal tissues with or without PPs. As presented in Fig. 2, in isolated intestinal tissues, the promotions on Ber permeation occured in all the SAA-PPs groups (SAA_L-PPs, SAA_M-PPs and SAA_H-PPs groups, $P < 0.01$) and in the SAA_H-NPPs group ($P < 0.05$). These results indicated that the promotive effects of SAA on Ber permeation in isolated intestinal tissues should be related to the participation of PPs.

3.4. SAA dynamically regulated PPs-associated intestinal immune microenvironment

Fig. 3 showed the effects of SAA on the mRNA expression of T-bet, STAT-6, ROR-γt and Foxp3 in PPs. There was no significant difference between NC group and BC group ($P > 0.05$). Compared with NC group, the administration of SAA dose-dependently upregulated the mRNA expressions of all these four kinds of transcription factors in SAA groups ($P < 0.05$). However, they exhibited different change curves. The up-regulation of SAA on STAT-6 and Foxp3 mRNA expression reached the highest level at 30 min after incubation, and gradually decreased with the extension of time. The up-regulation of SAA on T-bet and ROR-γt mRNA expression increased with the extension of time, reached the highest level at 90 min after incubation, and then began to decline.

Fig. 4 showed the effects of SAA on the expression of IFN-γ, IL-4, IL-17 and TGF-β in PPs. The positive expressions of IFN-γ, IL-4, IL-17 and TGF-β followed the same trends as the expression levels of T-bet, STAT-6, ROR-γt and FoxP3, respectively. These results indicated that SAA could dynamically regulate the differentiation of T lymphocyte and the secretion of immune effectors in PPs.

3.5. SAA dynamically regulated expression of TJ protein between intestinal epithelium, with PPs participation

Based on above results, the mechanism of the promotion on Ber permeation was investigated in isolated small intestinal tissues with high concentration of SAA. Fig. 5 and Fig. S1 showed the effects of SAA on the expression level of TJ proteins between intestinal epithelium cells, with or without the participation of PPs. The TJ proteins distributed around the intestinal epithelium cells. There was no significant difference between the BC group and the NC group ($P > 0.05$), with or without the participation of PPs. Compared with NC group, the SAA_H group without PPs (SAA_H-NPPs group) exhibited a degree of inhibition on ZO-1 and Claudin-1 expressions ($P < 0.05$) and no obvious effects on Occludin expression ($P > 0.05$), however, the SAA_H group with PPs (SAA_H-PPs group) exhibited gradually enhanced inhibition on the expressions of all the TJ proteins ($P < 0.01$). The above results indicated that SAA could dynamically regulate the expression of TJ proteins between intestinal epithelium cells, and PPs involved in this process.

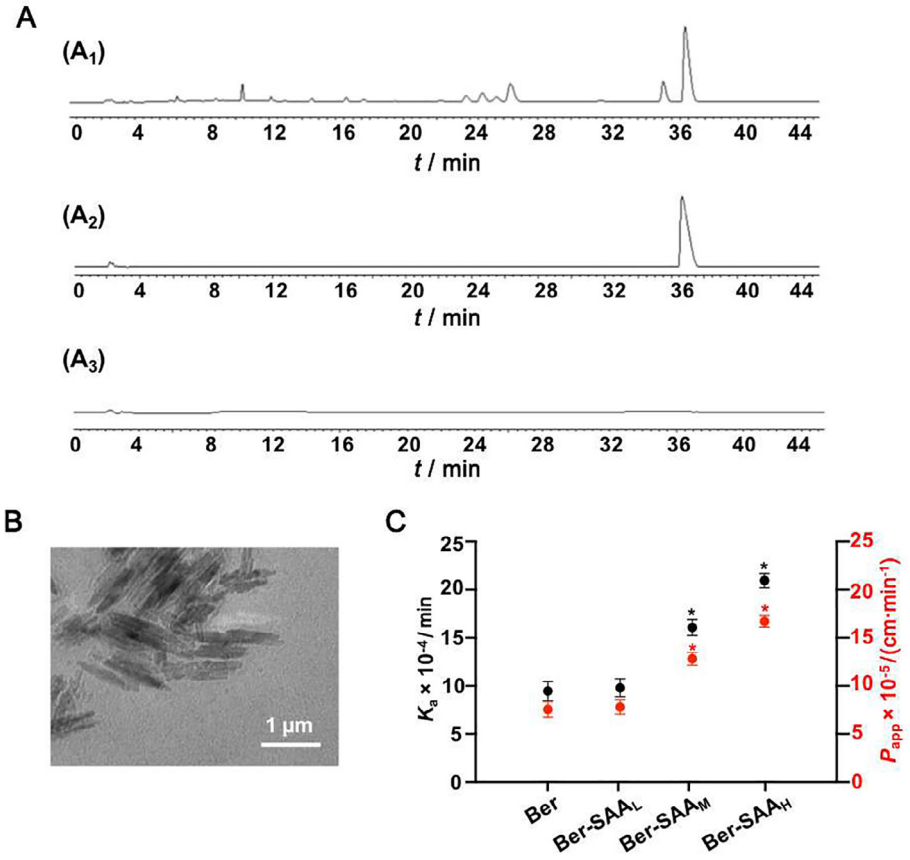

Fig. 1. SAA significantly affected Ber absorption in small intestine. (A) HPLC chromatograms of *Coptidis Rhizoma* decoction (A_1), Ber solution (A_2) and SAA suspension (120 μg/mL) (A_3). (B) Representative TEM image of SAA. (C) K_a and P_{app} variations of Ber absorption in the *in situ* intestinal perfusion model with different SAA concentrations. The data are expressed as mean ± SD (n = 5); $^{*}P < 0.05$, $^{**}P < 0.01$ and $^{***}P < 0.001$ *vs* Ber group.

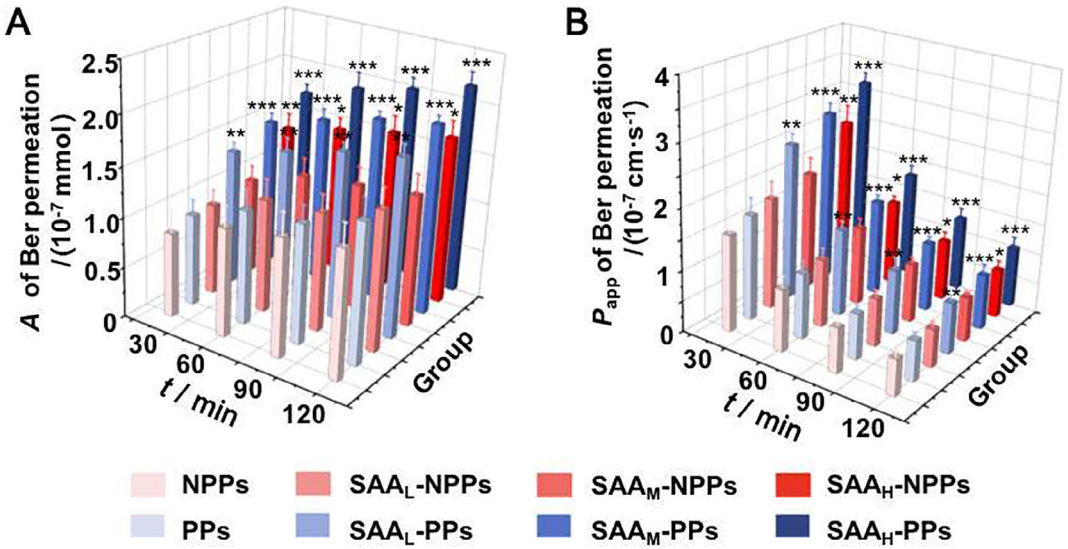

Fig. 2. SAA significantly affected Ber permeation in isolated intestinal tissue with PPs participation. A (A) and P_{app} (B) of Ber permeation in isolated intestinal tissue models with different SAA concentrations. The data are expressed as mean ± SD (n = 5); $^{*}P < 0.05$, $^{**}P < 0.01$ and $^{***}P < 0.001$ *vs* NPPs group at the same time point.

3.6. SAA significantly affected permeability of intestinal epithelium cells through PPs activation

To clarify the correlation between the PPs-associated immunity and the SAA-induced permeability increasing of intestinal epithelium cells, the influences of SAA on TJ proteins and Flu permeability were further investigated on the jejunum tissues with PPs_{IP}. Fig. 6A showed the effects of SAA on Flu permeability in jejunum tissues with the participation of PPs_{IP}. There was no significant difference between the PPs and PPs_{IP} groups ($P > 0.05$). The promotions on Flu permeation occured in all the SAA-PPs groups (SAA_L-PPs, SAA_M-PPs and SAA_H-PPs groups, $P < 0.01$) and in the SAA_M-PPs_{IP} and SAA_H-PPs_{IP} groups ($P < 0.05$). Compared with those in PPs groups, the promotive effects of SAA on Flu permeation in PPs_{IP}

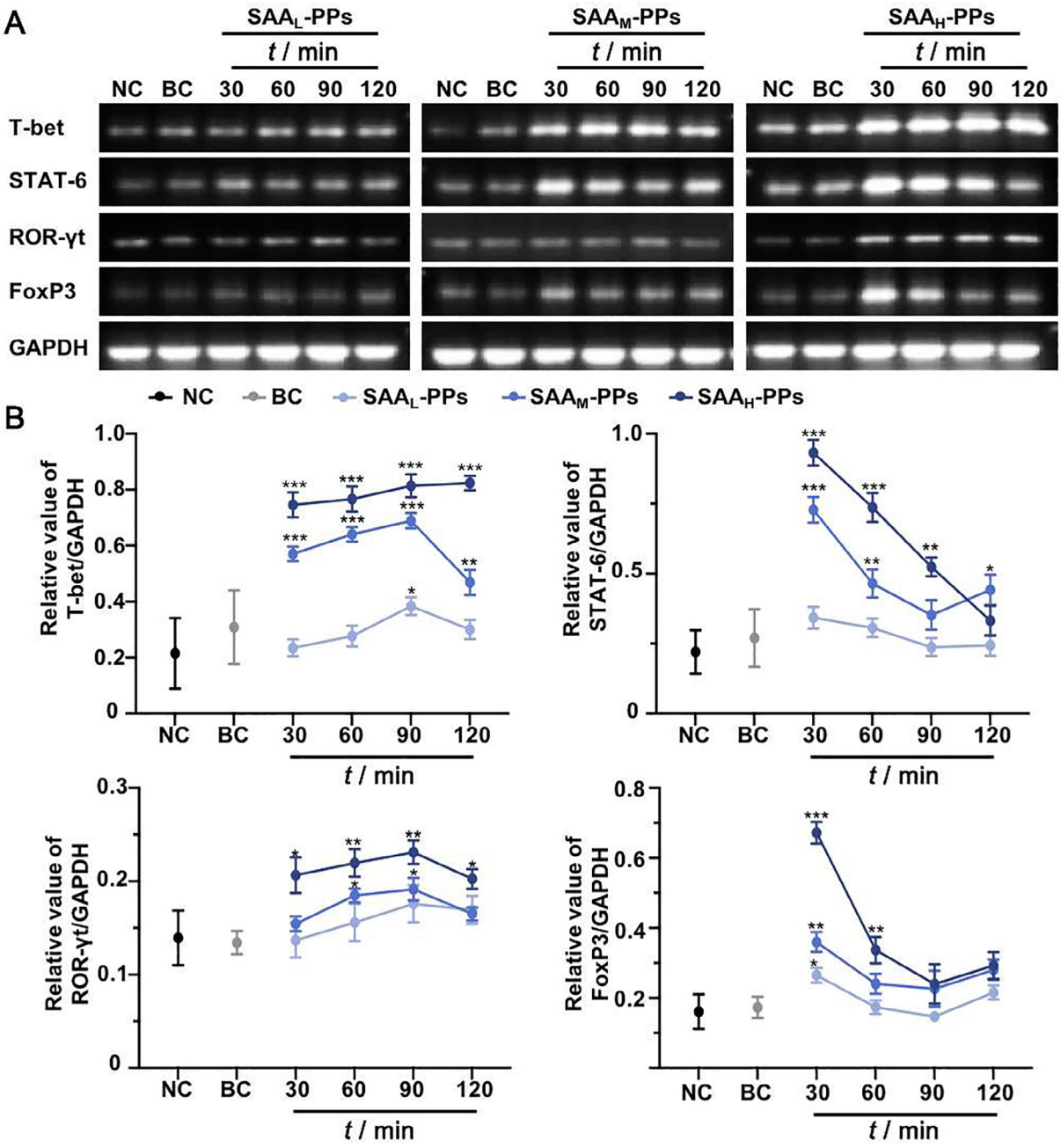

Fig. 3. SAA dynamically regulated expression levels of T-bet, STAT-6, ROR-γt and FoxP3 in PPs. (A) Representative agarose gel electrophoresis images of the RT-PCR analyses of T-bet, STAT-6, ROR-γt and FoxP3 expression in PPs at 30, 60, 90 and 120 min after SAA administration, compared with which in groups NC and BC. (B) Change curves of T-bet, STAT-6, ROR-γt and FoxP3 expression in PPs, in groups NC, BC, SAA$_L$-PPs, SAA$_M$-PPs and SAA$_H$-PPs, respectively. The data are obtained from five agarose gel electrophoresis images of the RT-PCR analyses. $^{*}P < 0.05$, $^{**}P < 0.01$ and $^{***}P < 0.001$ *vs* NC group.

groups was weakened ($P > 0.05$). Fig. 6B and Fig. S2 showed the effects of SAA$_H$ on the expressions of the TJ proteins ZO-1, Occludin and Claudin-1, with the participation of PPs or PPs$_{IP}$. Compared with the BC group, the ZO-1, Occludin and Claudin-1 expression in SAA$_H$-PPs$_{IP}$ group had been inhibited ($P < 0.05$). However, compared with the PPs groups, the inhibitory effects of SAA$_H$ on TJ proteins in PPs$_{IP}$ groups were weakened ($P < 0.05$). The above results indicated that the SAA-induced promotion on intestinal tissue permeability was associated with the activation of PPs.

4. Discussion

The dosage form of decoction has been used in clinic for centuries and well proved to be superior to single active component, but the mechanism underlying is still unclear. Most of the researches on decoction focus on the chemical changes of active ingredients, the chemical reactions between active ingredients, and the solubilization of amphiphilic molecules (Weng, Cai, Zhang, & Wang, 2019). The amphiphilic biomacromolecules in her-

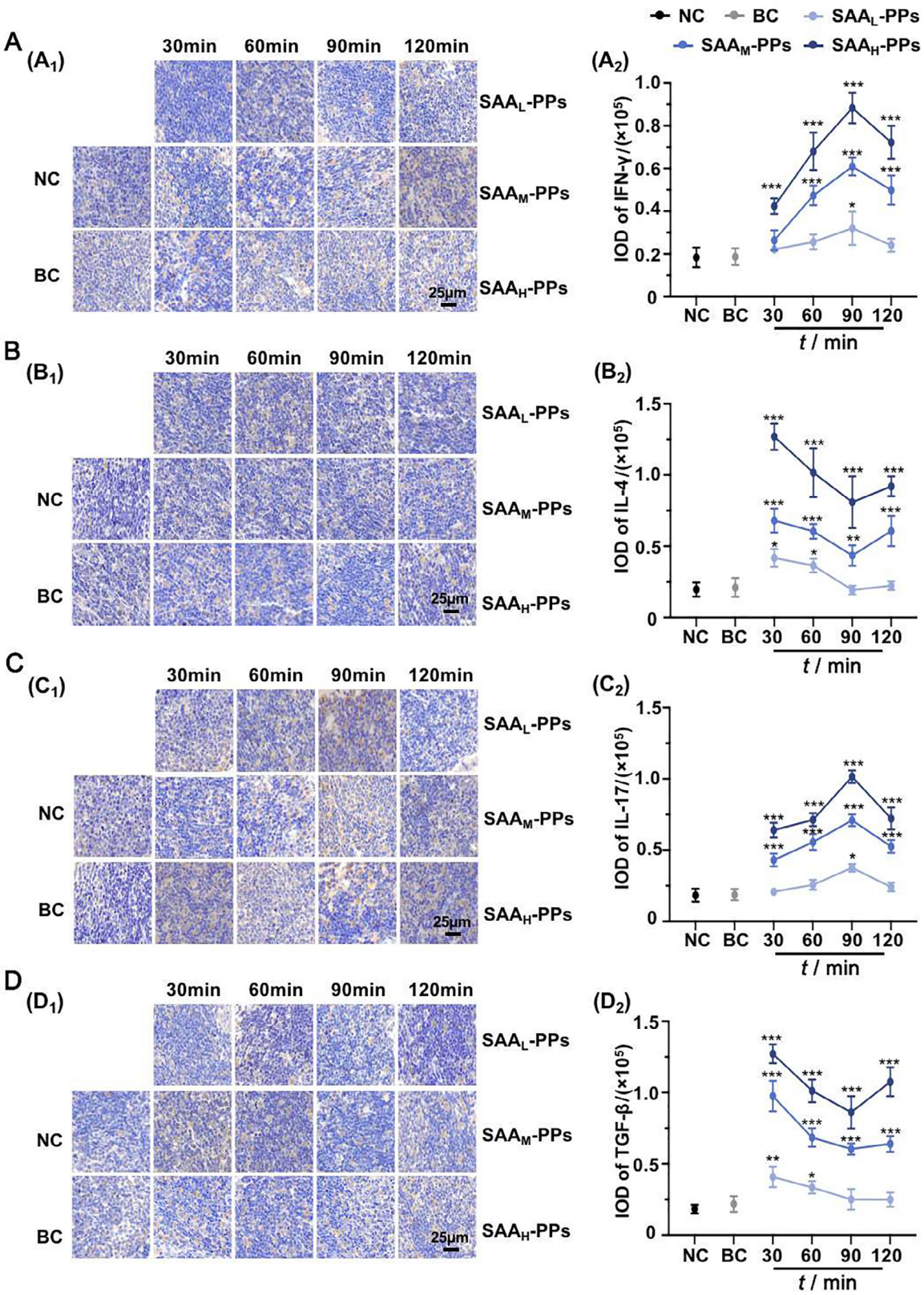

Fig. 4. SAA dynamically regulated secretion of IFN-γ, IL-4, IL-17 and TGF-β in PPs. Representative immunohistochemistry staining images (A1-D1) and IOD analyses (A2-D2) of IFN-γ (A), IL-4 (B), IL-17 (C) and TGF-β (D) expression in PPs at 30, 60, 90 and 120 min after incubation with SAA, compared with which in groups NC and BC. Original magnification × 200. The data are expressed as mean ± SD (n = 5), with data obtained from 10 randomly selected fields in immunohistochemistry sections. $^{*}P < 0.05$, $^{**}P < 0.01$ and $^{***}P < 0.001$ *vs* NC group.

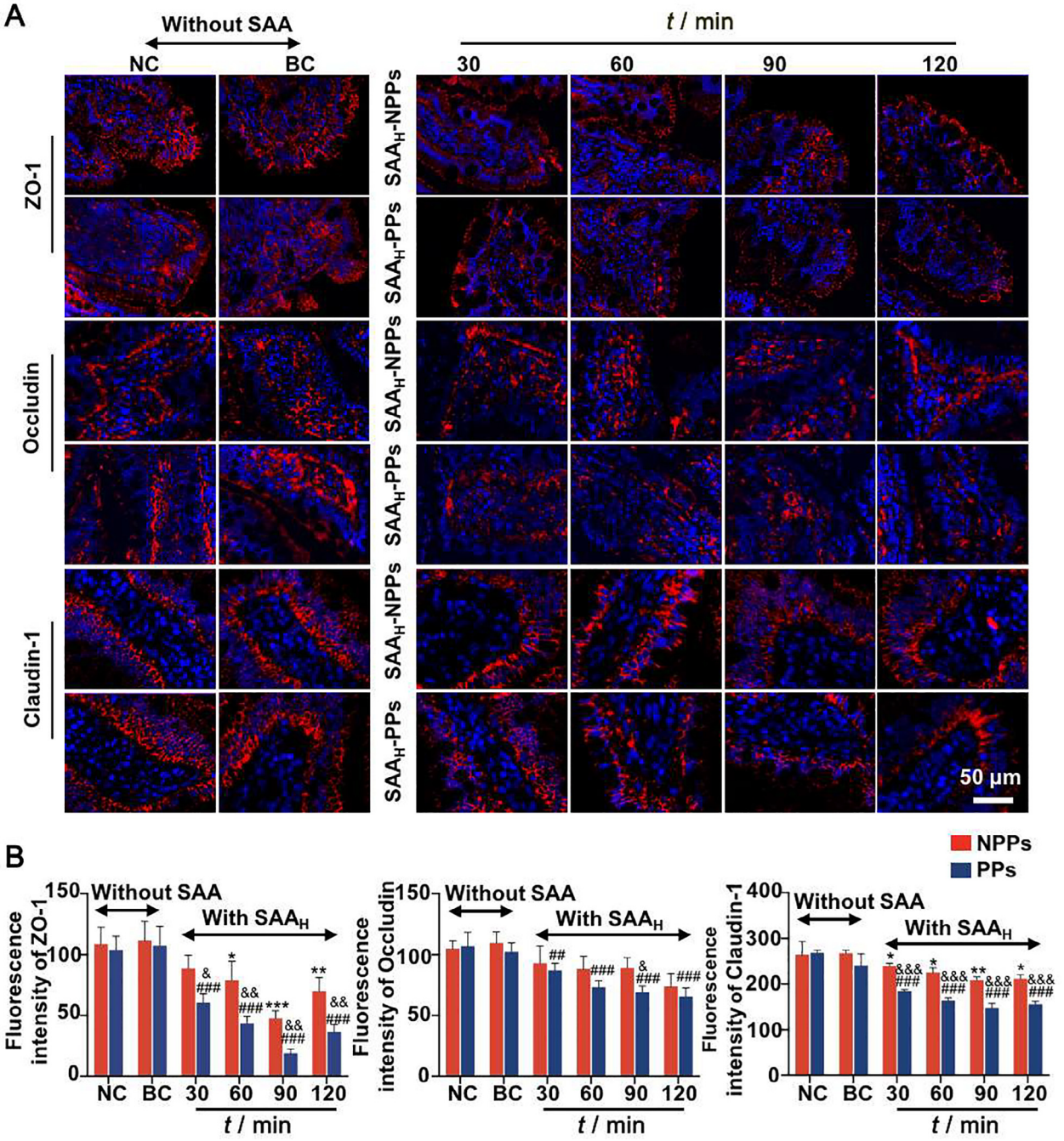

Fig. 5. Effects of SAA on expression of TJ proteins ZO-1, Occludin and Claudin-1 between intestinal epithelium cells, with or without participation of PPs. (A) Representative images of immunofluorescence staining TJ proteins ZO-1, Occludin and Claudin-1 (red) in intestinal villi, with nuclei stained by DAPI (blue). (B) IOD analyses of the expression levels of TJ proteins in each experimental group. Original magnification × 200. The data are expressed as mean ± SD (n = 5), with data obtained from 10 randomly selected fields in immunofluorescence sections. $^{*}P < 0.05$, $^{**}P < 0.01$ and $^{***}P < 0.001$ *vs* NC group without PPs participation; $^{\#}P < 0.05$, $^{\#\#}P < 0.01$ and $^{\#\#\#}P < 0.001$ *vs* NC group with PPs participation; $^{\&}P < 0.05$, $^{\&\&}P < 0.01$ and $^{\&\&\&}P < 0.001$ *vs* SAA$_H$-NPPs group at the same time point.

bal medicines (mainly of polysaccharides) dissolve out during the decocting process and spontaneously form into colloidal aggregations during cooling and standing (Liu & Huang, 2019; Shi et al., 2018; Su, Kan, Xie, Hu, & Pang, 2016). Previous researches have reported that these colloidal aggregations were closely related to the curative effects of the Chinese medicine decoction (Lü et al., 2018; Zhuang et al., 2008). *Coptidis Rhizoma* has multiple pharmacological effects on hypertension, hyperlipidemia, enteritis (Wang et al., 2019; Xiao et al., 2020; Zhang et al., 2011), etc, and has been widely used in clinic. Previous studies showed that the intestinal permeability coefficient of Ber in *Coptidis Rhizoma* decoction was significantly higher than that of Ber solution. Is this phenomenon related to the colloidal aggregations in the *Coptidis Rhizoma* decoction?

In the present study, it was firstly proved the significantly improvement of SAA on Ber absorption in intestinal perfusion experiment. The previous researches of our research group showed that the SAA was mainly composed of polysaccharides. Polysaccharides can be uptaken by the M cells on the surface of PPs in small intestine (Rathan et al., 2019). In order to avoid the influence of

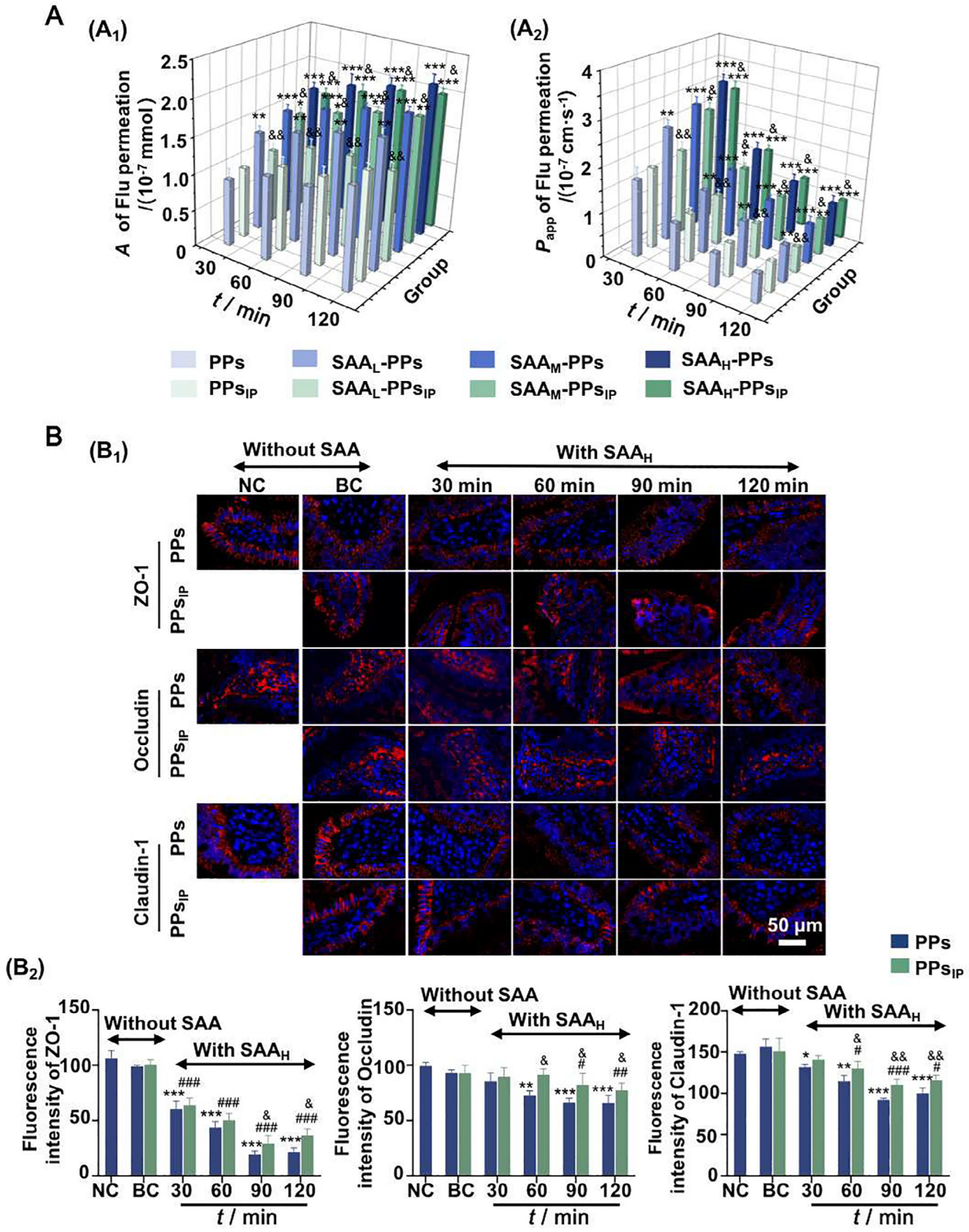

Fig. 6. SAA significantly affected permeability between intestinal epithelium cells through PPs activation. (A) A (A_1) and P_{app} (A_2) values of Flu permeation in isolated intestinal tissues with SAA incubated PPs or PPs_{IP}. (B) Representative fluorescent images of TJ proteins (red) in intestinal villi (B_1) and the quantitative analyses of the IOD (B_2), with nuclei stained by DAPI (blue). Original magnification × 200. The data are expressed as mean ± SD (n = 5). $^{*}P < 0.05$, $^{**}P < 0.01$ and $^{***}P < 0.001$ *vs* BC group with PPs participation; $^{\#}P < 0.05$, $^{\#\#}P < 0.01$ and $^{\#\#\#}P < 0.001$ *vs* BC group with PPs_{IP} participation; $^{\&}P < 0.05$, $^{\&\&}P < 0.01$ and $^{\&\&\&}P < 0.001$ *vs* PPs group at the same time point.

intestinal flora on the immune effect of intestinal PPs, an Ussing Chamber system was used to investigate whether PPs participated the promoting effects of SAA on Ber permeation in small intestine. The results showed that, SAA could dose-dependently increase Ber permeation in isolated small intestine tissues with the presence of PPs. However, when PPs was absent, the promotion of Ber permeation only appeared in group with high SAA concentration. These phenomena confirm the participation of PPs in the SAA promoting Ber permeation.

The TJ structure among cells is a multifunctional complex and is composed of various proteins. It is the structural basis of substance transport through paracellular pathway, and has the function of "barrier" and "fence" (Lin et al., 2019). The proteins ZO-1, Occludin and Claudin-1 are important protein molecules that constitute the TJ between cells and decide the permeability of intestinal tissues (Gong et al., 2017; Xie et al., 2019). With the participation of PPs, the expression level of all these TJ proteins was down-regulated by SAA in some extent. Moreover, these inhibitive effects change with the extension of time, indicating that the regulation of SAA on TJ was dynamic. In addition, because of the uneven distribution of bacteria in the whole intestinal lumen, the properties of local microenvironment drive variation in both identity and abundance of taxa (Tropini, Earle, Huang, & Sonnenburg, 2017). In the small intestine, where transit is faster, and simple sugar and amino acid metabolism is favored, the community is dominated by rapidly dividing facultative anaerobes such as Proteobacteria and Lactobacillales (Gu et al., 2013). Thus, SAA should not induce the invasion of harmful bacteria in the small intestine.

The promotive effects of SAA on Ber permeation in small intestine and the dynamic regulations of SAA on TJ between intestinal epithelium cells could be clearly observed in the experimental groups with PPs, which indicated that the above effects might be associated with PPs. M cells in PPs have the unique ability to present antigens, macromolecules and particles to lymphocytes and are considered to be helpful in initiating mucosal immunity. During the 120 min incubation with SAA suspensions, the mRNA expression of T-bet and ROR-γt in PPs increased continuously and the increasing of STAT-6 and Foxp3 expression was transient, indicating that SAA provided dynamic differentiation regulations of T lymphocytes. The secretion of immune effectors from differentiated T lymphocytes exhibited the similar variations. The balance of differentiated Th1, Th2, Th17 and Treg cells has been reported to be a major influence factor in intestinal function, as well as the immune effectors secreted by them (Chen et al., 2019; Xu et al., 2019). Thus, it was presumed that the SAA in *Coptidis Rhizoma* decoction could dynamically regulate the T lymphocytes differentiation in PPs and the secretion of various immune effectors after uptaken by M cells, then dynamically regulated the TJ between intestinal epithelium cells and promoted the Ber absorption/permeation in small intestine. In order to verify the correlation between PPs activation and the intestine tissue permeability, the TJ structure and Flu permeation of small intestine tissues were evaluated after incubation with PPs_{IP} and SAA, in an Ussing Chamber system. It could be seen that the PPs_{IP} groups with medium and high concentrations of SAA could dynamic regulate the TJ of isolated intestinal tissues and significantly promote Flu permeation. Combined with the proved regulation of SAA on PPs-associated immunity in above sections, these results indicated that SAA could significantly promote the permeability of intestinal epithelium cells through PPs activation.

Intestine research is a field of great biological complexity (Aarnoutse et al., 2019). Intestinal absorption of TCM decoction is affected by many factors, such as intestinal immunity, intestinal flora, intestinal peristalsis and so on. This study is limited to discussing PPs-related immunity. The results of this study indicated that the promotion effect on active ingredients absorption was related to the immune activity of SAA on PPs, but the specific mechanism of immune activation is not clear. Therefore, it is unclear whether this function of regulating intestinal epithelium permeability through immune activation is applicable to the absorption of active ingredients of other TCM decoctions.

5. Conclusion

The present study found that SAA could dynamically regulated the permeability of intestinal tissues and the structure of TJ between intestinal epithelium cells through activating the PPs-associated immunity. This may be one of the reasons why *Coptidis Rhizoma* decoction always has better biological activity than Ber solution administrated alone. Although our research results cannot explain the influence of colloidal aggregations in different TCM decoctions on the intestinal absorption of different active ingredients, it provides a theoretical and applied basis for the development of TCM dosage formulations from a new perspective.

Declaration of Competing Interest

The authors declare that they have no known competing financial interests or personal relationships that could have appeared to influence the work reported in this paper.

Acknowledgements

This work was supported by the National Natural Science Foundation of China (grant numbers 81874348, 81303239), the Natural Science Foundation of Anhui Province (grant numbers 1908085J29), the Key Research and Development Plan of Anhui Province (grant number 201904b11020023), the Open Project of State Key Laboratory of Natural Medicines (grant number SKLNMKF202007), the Provincial Foundation for Excellent Young Talents of Colleges and Universities of Anhui Province (grant number gxyqZD2018052), and the Anhui Provincial Department of Education (grant number KJ2018A0282).

Appendix A. Supplementary data

Supplementary data to this article can be found online at https://doi.org/10.1016/j.chmed.2021.06.004.

References

Aarnoutse, R., Ziemons, J., Penders, J., Rensen, S. S., de Vos-Geelen, J., & Smidt, M. L. (2019). The clinical link between human intestinal microbiota and systemic cancer therapy. *International Journal of Molecular Sciences, 20*(17), 4145.

Biundo, A., Reich, J., Ribitsch, D., & Guebitz, G. M. (2018). Synergistic effect of mutagenesis and truncation to improve a polyesterase from *Clostridium botulinum* for polyester hydrolysis. *Scientific Reports, 8*, 3745.

Brayden, D. J., Jepson, M. A., & Baird, A. W. (2005). Keynote review: Intestinal Peyer's patch M cells and oral vaccine targeting. *Drug Discovery Today, 10*(17), 1145–1157.

Chen, Y. F., Zheng, J. J., Qu, C., Xiao, Y., Li, F. F., Jin, Q. X., ... Jin, D. (2019). Inonotus obliquus polysaccharide ameliorates dextran sulphate sodium induced colitis involving modulation of Th1/Th2 and Th17/Treg balance. *Artificial Cells, Nanomedicine Biotechnology, 47*(1), 757–766.

Deng, X., & Song, X. Q. (2019). Comparison of efficacy between drug use regimens based on PK/PD parameters of berberine and clinical conventional regimens. *Chinese Journal of Rational Drug Use, 16*, 37–40.

Filipp, D., Brabec, T., Vobořil, M., & Dobeš, J. (2019). Enteric α-defensins on the verge of intestinal immune tolerance and inflammation. *Seminars Cell Developmental Biology, 88*, 138–146.

Gong, J., Hu, M., Huang, Z., Fang, K., Wang, D., Chen, Q., & Lu, F. (2017). Berberine attenuates intestinal mucosal barrier dysfunction in type 2 diabetic rats. *Frontiers Pharmacology, 8*.

Gu, S. H., Chen, D. D., Zhang, J. N., Lv, X. M., Wang, K., Duan, L. P., & Wu, X. L. (2013). Bacterial community mapping of the mouse gastrointestinal tract. *PLoS ONE, 8* e74957.

Gu, P. F., Liu, Z. G., Sun, Y. Q., Ou, N., Hu, Y. L., Liu, J. G., & Wang, D. Y. (2019). *Angelica sinensis* polysaccharide encapsulated into PLGA nanoparticles as a vaccine

delivery and adjuvant system for ovalbumin to promote immune responses. *International Journal of Pharmaceutics, 554*, 72–80.
Guo, L., Hong, D., Wang, S., Zhang, F., Tang, F., Wu, T., ... Liu, K. (2019). Therapeutic protection against *H. pylori* infection in mongolian gerbils by oral immunization with a tetravalent epitope-based vaccine with polysaccharide adjuvant. *Frontiers Immunology, 10*, 1185.
Huang, J., Guo, L., Tan, R., Wei, M., Zhang, J., Zhao, Y., ... Qiu, X. (2018). Interactions between emodin and efflux transporters on rat enterocyte by a validated Ussing chamber technique. *Frontiers Pharmacology, 9*.
Huang, Y., Ma, S., Wang, Y., Yan, R., Wang, S., Liu, N., ... Liu, L. i. (2019). The role of traditional Chinese herbal medicines and bioactive ingredients on ion channels: A brief review and prospect. *CNS & Neurological Disorders-Drug Targets, 18*(4), 257–265.
Huang, J., Zhang, J., Bai, J., Xu, W., Wu, D., & Qiu, X. (2016). LC-MS/MS determination and interaction of the main components from the traditional Chinese drug pair Danshen-Sanqi based on rat intestinal absorption. *Biomedical Chromatography, 30*(12), 1928–1934.
Jiang, Y., Li, X., Wu, Y., Zhou, L., Wang, Z., & Xiao, W. (2019). Effect of Lentinan on Peyer's patch structure and function in animmunosuppressed mouse model. *International Journal of Biological Macromolecules, 137*, 169–176.
Jiao, F., Hou, Z. Y., Yin, D. K., Yang, Y., & Gui, S. Y. (2016). Effect of solid particles in *Coptis* decoction on intestinal absorption of berberine *in situ*. *Chinese Traditional and Herbal Drugs, 47*, 1357–1360.
Li, C. L., Tan, L. H., Wang, Y. F., Luo, C. D., Chen, H. B., Lu, Q., ... Su, Z. R. (2019). Comparison of anti-inflammatory effects of berberine, and its natural oxidative and reduced derivatives from *Rhizoma Coptidis in vitro* and *in vivo*. *Phytomedicine, 52*, 272–283.
Li, H., Jin, H. E., Shim, W. S., & Shim, C. K. (2012). An improved prediction of the human *in vivo* intestinal permeability and BCS class of drugs using the *in vitro* permeability ratio obtained for rat intestine using an Ussing chamber system. *Drug Development and Industrial Pharmacy, 39*, 1515–1522.
Lin, J. C., Wu, J. Q., Wang, F., Tang, F. Y., Sun, J., Xu, B., ... Liang, J. (2019). QingBai decoction regulates intestinal permeability of dextran sulphate sodium-induced colitis through the modulation of notch and NF-κB signalling. *Cell Proliferation, 52*(2), e12547.
Liu, Y., & Huang, G. (2019). Extraction and derivatisation of active polysaccharides. *Journal of Enzyme Inhibition and Medicinal Chemistry, 34*(1), 1690–1696.
Liu, C., Luo, J., Xue, R.-Y., Guo, L., Nie, L., Li, S., ... Li, H.-B. (2019). The mucosal adjuvant effect of plant polysaccharides for induction of protective immunity against helicobacter pylori infection. *Vaccine, 37*(8), 1053–1061.
Lü, S. W., Su, H., Sun, S., Guo, Y. Y., Liu, T., Ping, Y., & Li, Y. J. (2018). Isolation and characterization of nanometre aggregates from a Bai-Hu-Tang decoction and their antipyretic effect. *Scientific Reports, 8*, 12209.
Meng, F. C., Wu, Z. F., Yin, Z. Q., Lin, L. G., Wang, R., & Zhang, Q. W. (2018). *Coptidis Rhizoma* and its main bioactive components: Recent advances in chemical investigation, quality evaluation and pharmacological activity. *Chinese Medicine, 13*, 13.
Rathan, J. K., Anneli, S., Adi, B., Jakob, C., Cristina, L. F., Neil, M., ... Nils, L. (2019). Activated Peyer's patches B cells sample antigen directly from M cells in the subepithelial dome. *Nature Communications, 10*, 1–15.
Shi, P., Lin, X., & Yao, H. (2018). A comprehensive review of recent studies on pharmacokinetics of traditional Chinese medicines (2014–2017) and perspectives. *Drug Metabolism Reviews, 50*(2), 161–192.
Su, B., Kan, Y. J., Xie, J. W., Hu, J., & Pang, W. S. (2016). Relevance of the pharmacokinetic and pharmacodynamic profiles of *Puerariae Lobatae Radix* to aggregation of multi-component molecules in aqueous decoctions. *Molecules, 21*, 845.
Sun, A. H., Gu, J., Wu, T., Yuan, Z. K., Cai, X., Hu, Z. X., Jian, W. X., & Li, X. (2016). Impact of four anesthetic drugs commonly used in animal experiments on the cardiovascular system in rats. *Acta Laboratorium Animalis Scientia Sinica, 24*, 120–126.
Tropini, C., Earle, K. A., Huang, K. C., & Sonnenburg, J. L. (2017). The gut microbiome: Connecting spatial organization to function. *Cell Host & Microbe, 21*(4), 433–442.
Wang, M., Meng, X. Y., Yang, R. L., Qin, T., Wang, X. Y., Zhang, K. Y., Fei, C. Z., Li, Y., Hu, Y. L., & Xue, F. Q. (2012). *Cordyceps militaris* polysaccharides can enhance the immunity and antioxidation activity in immunosuppressed mice. *Carbohydrate Polymers, 89*(2), 461–466.
Wang, J., Wang, L., Lou, G. H., Zeng, H. R., Hu, J., Huang, Q. W., Peng, W., & Yang, X. B. (2019). *Coptidis Rhizoma*: A comprehensive review of its traditional uses, botany, phytochemistry, pharmacology and toxicology. *Pharmaceutical Biology, 57*, 193–225.
Weng, Q., Cai, X., Zhang, F., & Wang, S. (2019). Fabrication of self-assembled *Radix Pseudostellariae* protein nanoparticles and the entrapment of curcumin. *Food Chemistry, 274*, 796–802.
Xiao, S. W., Liu, C., Chen, M. J., Zou, J. F., Zhang, Z. M., Cui, X., Jiang, S., Shang, E., Qian, D. W., & Duan, J. A. (2020). *Scutellariae Radix* and *Coptidis Rhizoma* ameliorate glycolipid metabolism of type 2 diabetic rats by modulating gut microbiota and its metabolites. *Applied Microbiology and Biotechnology, 104*(1), 303–317.
Xie, S. Z., Liu, B., Ye, H. Y., Li, Q. M., Pan, L. H., Zha, X. Q., Liu, J., Duan, J., & Luo, J. P. (2019). Dendrobium huoshanense polysaccharide regionally regulates intestinal mucosal barrier function and intestinal microbiota in mice. *Carbohydrate Polymers, 206*, 149–162.
Xu, M., Duan, X. Y., Chen, Q. Y., Fan, H., Hong, Z. C., Deng, S. J., ... Zhou, C. Z. (2019). Effect of compound sophorae decoction on dextran sodium sulfate (DSS)-induced colitis in mice by regulating Th17/Treg cell balance. *Biomedicine & Pharmacotherapy, 109*, 2396–2408.
Xu, H. H., Yang, Y., Chen, Q. Q., Ren, R. R., Yin, D. K., & Gui, S. Y. (2018). Effect of *Coptis chinensis* water decoction microparticle system on tight junction structure and expression of tight junction protein ZO-1 in intestinal epithelial cells of rats. *Anhui Traditional Chinese Medical College, 37*, 64–68.
Xue, J., Tong, S., Wang, Z., & Liu, P. (2018). Chemical characterization and hypoglycaemic activities *in vitro* of two polysaccharides from *Inonotus Obliquus* by submerged culture. *Molecules, 23*(12), 3261.
Yang, H. J., Kim, M. J., Kang, H. J., Lee, H. Y., & Park, K. H. (2018). Immunomodulating properties of *Polygonum multiflorum* extracts on cyclophosphamide-induced immunosuppression model. *Indian Journal of Pharmaceutical Sciences, 80*, 749–754.
Yang, Y., Li, Y., Yin, D., Chen, S., & Gao, X. (2016). *Coptis chinensis* polysaccharides inhibit advanced glycation end product formation. *Journal of Medicinal Food, 19*(6), 593–600.
Zhang, Q., Piao, X. L., Piao, X. S., Lu, T., Wang, D., & Kim, S. W. (2011). Preventive effect of *Coptis chinensis* and berberine on intestinal injury in rats challenged with lipopolysaccharides. *Food and Chemical Toxicology, 49*(1), 61–69.
Zhou, J., Wei, K., Wang, C., Dong, W., Ma, N., Zhu, L., ... Zhu, R. (2017). Oral immunisation with Taishan *Pinus massoniana* pollen polysaccharide adjuvant with recombinant Lactococcus lactis-expressing *Proteus mirabilis* ompA confers optimal protection in mice. *Allergologla et Immunopathologla, 45*(5), 496–505.
Zhuang, Y., Yan, J., Zhu, W., Chen, L., Liang, D., & Xu, X. (2008). Can the aggregation be a new approach for understanding the mechanism of traditional Chinese medicine? *Journal of Ethnopharmacology, 117*(2), 378–384.